

Magnitude of Corona Current Caused by Aircraft Net Charge

Xingya Da,* Huairong Shen,[†] and Lei Hong[‡]
*Academy of Equipment Command and Technology,
101416 Beijing, People's Republic of China*

DOI: 10.2514/1.39857

This paper presents a new method to estimate the corona current emitted from aircraft through calculating the electric field distribution around the corona point on the aircraft surface. Assuming the ion transition region to be a semisphere, the electric field distribution caused by the net charge in this semisphere is calculated based on the method of moments. The charge distribution in the semisphere is deduced by taking the field-distribution model into Poisson's equation for electrostatics, and then the corona-current model is established based on Ohm's law. By taking the wind speed of 30 m/s as the flight speed, the computational result of the approximate relation between wing-tip current and aircraft net charge for a TF-1 unmanned aerial vehicle is $I_s = 1.3815Q - 0.0062/Q$, where Q is the net charge in microcoulombs and I_s is the current in microampere. Works in this paper show that the magnitude of the corona current caused by aircraft net charge is almost proportional to the magnitude of net charge and aircraft flight speed.

I. Introduction

ATTEMPTS are currently underway for the application of the TF-1 unmanned aerial vehicle (UAV) to measure atmospheric electric field in our laboratory. TF-1 is the first-generation aero-exploration UAV of China designed to measure meteorological data such as wind speed, temperature, pressure, and humidity. Additional information on the evolving charge structure of electrified clouds can be obtained if TF-1 is used to measure the field. However, using aircraft to measure atmospheric electric field is heavily affected by aircraft corona emissions, which could cause errors of dozens of kilovolts per meter in extreme situations [1–3]. To relieve the corona effect on TF-1 electric field measurements, it is critical to study how the corona current affects the measurements in theory. It is easier for the aircraft net charge to trigger corona emissions than an ambient electric field in most flights [4], and so the first problem that needs to be solved is the establishment of the model of corona current caused by the net charge.

It must be noted that calculating the corona magnitude caused by the net charge is challenging due to the complex environment around an aircraft, the special electrodes on the aircraft surface, and the effect of wind. Previous calculation methods were mainly used for point and pin-plate corona emissions. For instance, Chapman [5] calculated the current from an isolated electrode. His method was based on a space-charge-limited equation that assumes that the charge areas are spheres. He established the model and validated it using a parabolic corona point that showed that the method was in good agreement with his experiment.

Considering that isolated instances are closer to the isolated flying aircraft, we present a new aircraft corona-current calculation method based on the space-charge-limited method at the wing tip of the TF-1. In our new method, however, we do not integrate Poisson's equation or turn the electric field into the derivative of the electric potential. Instead, we directly establish the field-distribution model in the ion transition region and calculate the corona current through Poisson's equation.

Received 18 July 2008; revision received 30 August 2008; accepted for publication 2 September 2008. Copyright © 2008 by the American Institute of Aeronautics and Astronautics, Inc. All rights reserved. Copies of this paper may be made for personal or internal use, on condition that the copier pay the \$10.00 per-copy fee to the Copyright Clearance Center, Inc., 222 Rosewood Drive, Danvers, MA 01923; include the code 0021-8669/09 \$10.00 in correspondence with the CCC.

*Postgraduate, Postgraduate College; Dxingya@gmail.com.

[†]Professor, Department of Aeronautics; Shenhuair@tom.com.

[‡]Postgraduate, Postgraduate College; Redleilei@163.com.

II. Computation Method

A. Corona-Current Computation Method

The space-charge-limited method divides the space into two regions: the ion transition region, seen as a sphere or cone near the point, and the rest space, in which there is no space charge. There is indeed a conducting plasma area that is roughly spherical in the immediate vicinity of the point. The limit of the plasma sphere extends to a radius r_p of about 0.01–0.04 cm, at which ionization by collision is appreciable. The plasma sphere is always neglected and seen as a part of the spherical ion transition region when calculating the corona current. The mobility of ions in this transition region determines the magnitude of the corona current.

By definition of mobility k in a field E , the velocity of ions is $u = kE$. According to Ohm's law, for charge density ρ on the shell of the ion transition region, the current I flowing through the shell is

$$I = sk\rho(r)E(r) \quad (1)$$

where s is the area of the shell. To calculate the current flowing through a semisphere, the area $s = 2\pi r^2$; if we calculate the current flowing through a sphere shell, the area $s = 4\pi r^2$. From Poisson's equation for electrostatics,

$$\frac{1}{r^2} \frac{d}{dr} (r^2 E) = \rho/\epsilon_0 \quad (2)$$

If the field distribution in the transition region is known, we use Poisson's equation to calculate ρ and bring it into Eq. (1) to calculate the current. We have

$$I = sk\epsilon_0 E(r) \frac{1}{r^2} \frac{d}{dr} (r^2 E) \quad (3)$$

In our method, we assume that the transition region is a semisphere and let its exterior radius be r_s . The current is calculated as

$$I_s = 2\pi k\epsilon_0 E(r) \frac{d}{dr} (r^2 E)|_{r=r_s} \quad (4)$$

B. Computation Method of Field Distribution

In previous computation methods, Eq. (4) was not used to compute corona current. Instead, integrating Eq. (3) and substituting E with the electric potential difference ΔV between the inner and outer semispheres was done. We can also establish the model of ΔV to calculate current. However, such methods neglect some insignificant

parts (see the details in [4]). In our proposed method, we calculate current by establishing directly the model of E . This process can involve more information.

We use our previous method based on the method of moments to compute the electric field. This method establishes the electric-field-enhanced factor model as

$$E = C \begin{bmatrix} E_x \\ E_y \\ E_z \\ Q \end{bmatrix} \quad (5)$$

where C is a fixed 3×4 electric-field-enhanced factor matrix; E_x , E_y , and E_z are the atmospheric electric field components in the aircraft body frame; and Q is the aircraft net charge (see the details in [4]).

By inserting the discrete electric field $E(r_i)$ along the radial direction, the field distribution model $E(r)$ can be quantified. To calculate the discrete field $E(r_i)$, then n equals the equidistant points on the semishell with radius r_i and the equidistant points' fields equal $E_j(r_i)$, where $j = 1:n$. Because n is uniformly distributed, the field $E(r_i)$ can be calculated by the mean value of $E_j(r_i)$. Thus,

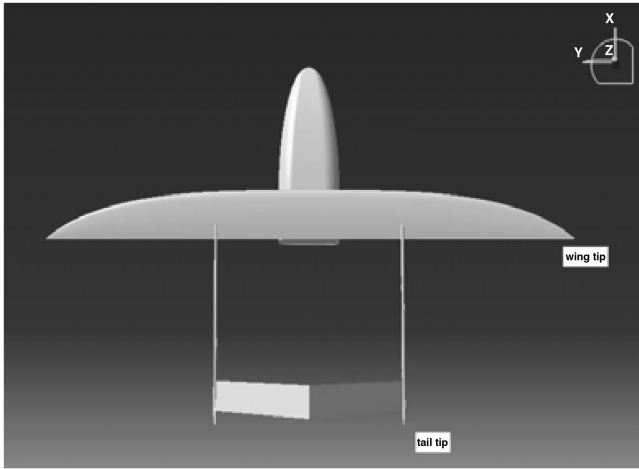
$$E(r_i) = \sum_{j=1}^n E_j \frac{r_i}{n}$$

When the model $E(r)$ is established, the corona current can be approximated by substituting it into Eq. (4).

III. Computation Results and Analysis

A. Wing-Tip Corona Current of the TF-1

Figure 1a shows the top view of the TF-1. Analysis on TF-1 shows that the wing tip is most likely to emit corona ions. Therefore, we



a)



b)

Fig. 1 TF-1 a) 3-D model and b) wing tip.

only calculate the corona current caused by the net charge at the wing tip. Figure 1b shows the top view of the wing tip.

From Eq. (5) in our method, the field strength caused by the net charge (see details in [4]) is

$$E = \sqrt{C_{14}^2 + C_{24}^2 + C_{34}^2} Q / 4\pi\epsilon_0 = aQ / 4\pi\epsilon_0$$

The strength is linear with $Q/4\pi\epsilon_0$, and so we only need to analyze the factor a .

Figure 2 plots the equipotentials at the wing tip in the x - y plane. The solid lines are the equipotentials, the dashed-dotted lines are presumed to be charge spheres, and the arrow indicates the direction of the wing-tip field. The values labeled on the equipotentials are the potentials in which the factor $Q/4\pi\epsilon_0$ is omitted. The figure shows that the equipotentials are almost symmetrical with the field direction line. Therefore, we choose the semisphere above the dashed line to calculate the current.

The fields of 121 points are calculated on each semisphere shell at an equal distance along the radial. The statistics are shown in Fig. 3. Figure 3a shows the variance of a in the 121 points on each shell; the solid line in Fig. 3b is the mean value of a along the radial. The relatively small variance compared with a indicates that the fields are almost equal on an equiradius semisphere shell. The assumption used by the space-charge-limited method that the field strength is only relevant with the radius is somehow correct. Incorporating the mean values, we have

$$E(r) = \frac{b}{r+c} \frac{Q}{4\pi\epsilon_0} = \frac{0.0921}{r+0.000277} \frac{Q}{4\pi\epsilon_0} \quad (6)$$

The fitting results are also showed in Fig. 3b (the dashed line). The variance of the fitting error is 0.6387.

Taking Eq. (6) into Eq. (4), the current can be expressed as

$$I = 2\pi k\epsilon_0 E(r_s) \frac{d}{dr} (r^2 E) = k \frac{b^2 r_s (r_s + c) Q^2}{8\pi (r_s + c)^3} \frac{Q^2}{\epsilon_0} \quad (7)$$

Note that all of the space is divided into two parts: the space-charge semisphere of radius r_s and all the rest of space in which there is no space charge. The space-charge semisphere is chosen to have a size that just encompasses the region in which ion motion is dominated by the electric field. Beyond the semisphere, the wind dominates the ion motion. To balance the viscous force with the electrical force, the ion speed could be regarded as being equal to the wind speed w . Note that this approximation does not mean that the charge outside the semisphere is determined by wind, but that the wind is a major factor. This is a reasonable approximation. Thus, r_s is chosen such that w is just equal to the ion speed in the outer shell of the charge transition region:

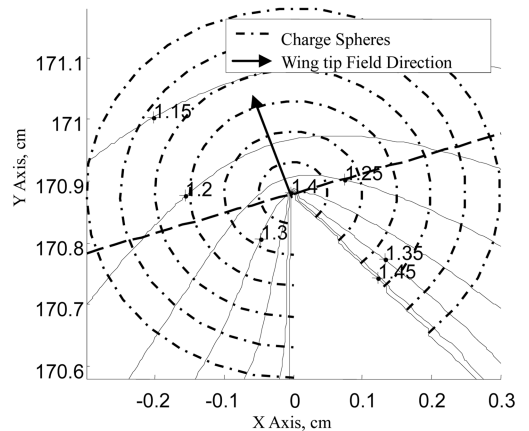


Fig. 2 Equipotentials at the wing tip of the TF-1.

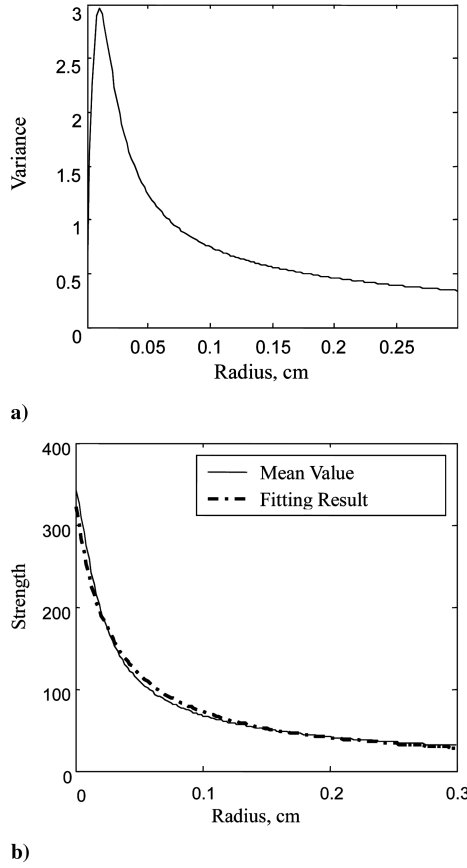


Fig. 3 Semisphere a) field variance and b) fitting result.

$$kE_s = w \quad (8)$$

The exterior radius of the semisphere is

$$r_s = \frac{kbQ}{4\pi w\epsilon_0} - c \quad (9)$$

Taking this equation into Eq. (7), the current

$$I_s = \frac{bw}{2} Q - \frac{8(\pi\epsilon_0 c)^2 w^3}{k^2 b Q} \quad (10)$$

Taking the mobility of $1.5 \times 10^{-4} \text{ m}^2 \cdot \text{s}^{-1} \cdot \text{V}^{-1}$ as an average value for ions at atmospheric pressure and w of 30 m/s as the maximum speed of the TF-1, then letting the unit of Q be in microcoulombs and the unit of I_s be in microampere, Eq. (10) can be simplified as

$$I_s = 1.3815Q - \frac{0.0062}{Q} \mu\text{A} \quad (11)$$

where $|Q| > 0.84 \mu\text{C}$. Obviously, $|Q| = 0.84 \mu\text{C}$ is the threshold that would trigger corona emissions at the wing tip when taking the corona breakdown strength as 2600 kV/m.

B. Discussion

Magnitude expression shows us that the corona current is almost proportional to the net charge. According to electronics laws, aircraft potential is also proportional to the net charge, for which the proportional factor is the aircraft's capacity. Thus, the corona current is proportional to the body potential in our results. According to other studies on corona current for pin-plate electrodes and other isolated electrodes, the relationship between body potential and current is

$$I = c \frac{V(V - V_0)}{r_s} \quad (12)$$

This relationship proposes that the current varies as the square of the potential. Nevertheless, Chapman [5] also indicates that r_s is proportional to the potential. Therefore, Eq. (12) can be turned into a linear format by establishing the model of r_s . Furthermore, Chapman also found that the corona current from an isolated point is proportional to the point potential [5,6] which is consistent with our result.

C. Aircraft Net Charge

Equation (11) shows that the magnitude of corona current due to the net charge is larger than the magnitude of the net charge. Corona current decreases the net charge, which also results in a decrease in corona magnitude. When the net charge is smaller than $0.84 \mu\text{C}$, a TF-1 will stop emitting corona ions. If surface charging cannot be sustained, the corona current only occurs in impulse. The corona magnitude is determined by the magnitude of the net charge, but whether the emission can be sustained is determined by the surface charging. For different charging rates, the net charge can reach different levels. If the charging rate is I_c , then we can find the balance state of the net charge by solving the following equation:

$$I_s = 1.3815Q - \frac{0.0062}{Q} = I_c \mu\text{A} \quad (13)$$

Taking I_c as $5 \mu\text{A}$, the balanced net charge is $3.619 \mu\text{C}$. We still do not have the charging-rate data on TF-1. According to previous studies, a general aircraft can charge $400 \mu\text{C}$ per second while penetrating thunderstorms [7]. Taking surface areas into consideration, we conservatively approximate that the charging rate of the TF-1 can run up to $10 \mu\text{A}$ in extreme situations. Taking this value into the current calculation model, the net charge can reach $7.23 \mu\text{C}$, a somewhat high level. Analysis shows that the tail tip of the TF-1 will emit corona ions when $|Q| > 2.4 \mu\text{C}$ [4]. Therefore, if the charging rate achieves the $10 \mu\text{A}$ level, the tail tip will emit corona ions too. This indicates that the corona effect on field measurements caused by the net charge may be rather complex.

IV. Conclusions

In this paper, the corona-current calculation model at the wing tip of the TF-1 is established based on space-charge-limited methods. At the core of this modeling process is the field calculation on the charge semisphere using our previous electric field computation method for aircraft. Calculation results show that the field in the charge semisphere is almost solely determined by the radius r in inverse proportion. This indicates that the choice of space-charge-limited method is correct. Taking the maximum flight speed of the TF-1 into consideration, the model is simplified to the sum of two parts: a major part being proportional to the net charge and an insignificant part being inversely proportional to the net charge. We can approximate corona current by directly taking the net charge into this model. This theoretical model lays the foundation for future studies on relieving the effect of aircraft corona emissions on electric field measurement.

References

- [1] Jones, J. J., Winn, W. P., and Han, F., "Electric Field Measurements with an Airplane: Problems Caused by Emitted Charge," *Journal of Geophysical Research*, Vol. 98, No. D3, 1993, pp. 5235–5244. doi:10.1029/92JD02686
- [2] Mo, Q., Ebner, E., Fleischhacker, P., and Winn, W. P., "Electric Field Measurements with an Airplane: A Solution to Problems Caused by Emitted Charge," *Journal of Geophysical Research*, Vol. 103, No. D14, 1998, pp. 17163–17173. doi:10.1029/98JD01149
- [3] Mo, Q., Feind, R. E., Kopp F. J., and Detwiler A. G., "Improved Electric Field Measurements with the T-28 Armored Research Airplane," *Journal of Geophysical Research*, Vol. 104, No. D20, 1999, pp. 24485–24497. doi:10.1029/1999JD900834
- [4] Da, X., Shen, H., and Hong, L., "New Electric Field Computation

- Method for Aircraft,” *Journal of Aircraft*, Vol. 46, No. 2, 2009, pp. 557–561.
doi:10.2514/1.38699
- [5] Chapman, S., “The Magnitude of Corona Point Discharge Current,” *Journal of the Atmospheric Sciences*, Vol. 34, No. 11, 1977, pp. 1801–1809.
doi:10.1175/1520-0469(1977)034<1801:TMOCPD>2.0.CO;2
- [6] Chapman, S., “Corona Point Current in Wind,” *Journal of Geophysical Research*, Vol. 75, No. 12, 1970, pp. 2165–2169.
doi:10.1029/JC075i012p02165
- [7] Jones, J. J., “Electric Charge Acquired by Airplanes Penetrating Thunderstorms,” *Journal of Geophysical Research*, Vol. 95, No. D10, 1990, pp. 16589–16600.
doi:10.1029/JD095iD10p16589